

# SEPTUM HORN ANTENNAS AT 47/48 GHz FOR HIGH ALTITUDE PLATFORM STATIONS

Z. Hradecky, P. Pechac, M. Mazanek, R. Galuscak

CTU Prague, FEE, Dept. of Electromagnetic Field, Technicka 2, 166 27 Prague, Czech Republic  
E-mail: hradecz@fel.cvut.cz, pechac@fel.cvut.cz, mazanekm@fel.cvut.cz, om6aa@yahoo.com

**Keywords:** Septum horn antenna, circular polarization, HAP

## Abstract

The septum horns are aperture type antennas with the possibility to offer a circular polarization. The antenna can use both polarizations (left- and right-hand circular - LHC, RHC) simultaneously at the same time. Circular polarization has advantages in providing different services, e.g. coverage from HAPs, where better power budget is obtained by minimizing the polarization loss. A design of a septum horn antenna for frequency band 47.0 – 48.5 GHz (based on the studies and designs at 1.3 GHz and 2.4 GHz) is presented in the paper; possibilities of the septum horn antenna design and available parameters are discussed. Thanks to the circular polarization and rotationally symmetrical aperture such antennas provide a pencil beam radiation pattern with a very low side lobes level. A 20 dBi gain septum horn antenna was developed and manufactured. Calculated data (radiation pattern, beamwidth, sidelobes suppression, gain and VSWR) were compared with measured data. Adaptations of the antenna design for possible deformations of the radiation pattern to get proper coverage footprint is discussed.

## 1 Introduction

High Altitude Platforms (HAPs) represents a future technology to deliver various communication services. HAP stations will be situated in a semi-stationary position in the stratosphere at an altitude of 17 – 22 km [4,7]. For broadband communications 47/48 GHz frequency band was allocated to HAPs in Europe [8]. Antennas are very important components in any wireless communications network. In HAP based systems very narrow antenna beams with low side lobe levels are required to provide a cellular coverage on the ground optimizing coverage and interference. Beamforming using antenna arrays is assumed. Mechanically steered horns are another option. A septum horn antenna is one of the candidate antenna technologies for HAP communication systems in this millimeter frequency band.

## 2 Septum horn

Frequently, to obtain the circular polarization, a circular waveguide excited by two orthogonal modes with 90 degree

phase shifted signals, is used. The 90 degree phase shift is produced by a “power hybrid divider” that must handle high power levels; thus, it is very sensitive to manufacturing tolerances and introduces unwanted attenuation (0.1 - 0.2 dB) as well.

Another popular septum polarization transformer employing a waveguide with square cross-section is frequently used [3]. The mismatch between the waveguide’s square shape and the inherently circular form of the electromagnetic field originating behind the septum introduces unwanted side lobes. Crosspolarization losses may be reduced somewhat by optimization of the septum transformer and choke designs. The above related problems can be solved by using a septum polarization transformer configured in a waveguide having a circular cross section (see Figure 1).

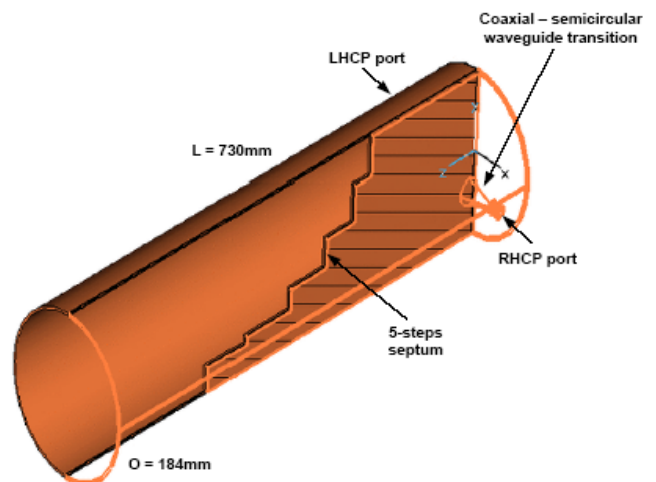


Figure 1: Proposed 1.3 GHz septum layout [5].

Because the structure is quite complex to perform a full-wave optimization directly, we divided its design into two somewhat independent steps:

1. Design of the 5-step septum in a circular waveguide using the Mician Microwave Wizard (MMW) [9]. This software utilizes fast modal matching technique [1], [2].
2. Design and adjustment of the coaxial-semicircular waveguide transition together with the septum by using the full-wave FIT method implemented in CST Microwave Studio (CST MWS).

Simulations in MMW (see Figure 2) were intended to achieve the maximum possible separation between the radiated LHC and RHC components by adjusting all parameters of the 5-step septum. The best separation obtained was about 50 dB.

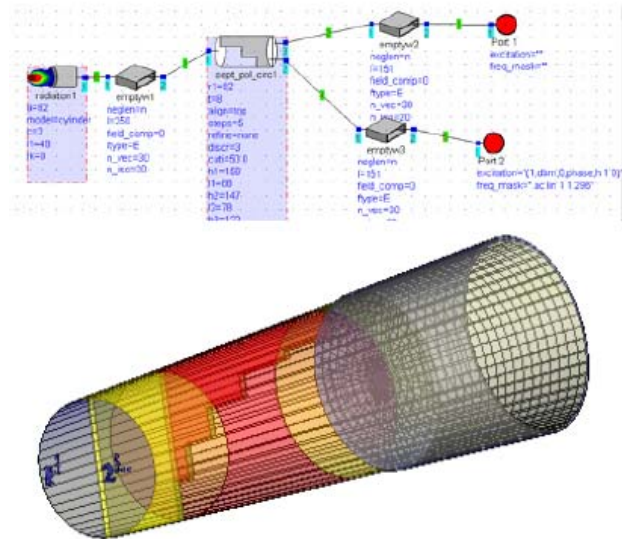


Figure 2: Simplified model for MMW analyses

Once the optimum dimensions of the 5-step septum were determined, the entire feed was simulated using CST MWS applied to the model in Figure 2. Electrical excitation of the waveguide was chosen because of its simplicity. Two probes were employed to match the waveguide's structure to the input coaxial line. Because of the structure's symmetry ( $S_{11} = S_{22}$ ,  $S_{12} = S_{21}$ ), simulation of only one port was necessary. The optimization strategy used was to determine the probe parameters leading to the best matching and isolation between ports.

### 2.1 Septum for 47 - 48.5 GHz frequency band

Waveguide design with septum inside was based on experience with design at 1.3 GHz [5]. Circular waveguide diameter is close to the maximum (5 mm) to the cut-off frequency of second (higher) mode. Input coaxial waveguide dimensions come out from the 2.4 mm connector. Optimization performed was based on: probe diameter, probe length, distance between probe and short and septum dimensions. Optimization criteria were port: impedance matching better than -20 dB and port isolation better than -25 dB. Optimized dimensions are: diameter of excitation probe 1.15 mm, probe length 0.65 mm and distance between probe and short 0.3 mm. Designed waveguide with septum is depicted in Figure 3.

Figure 9 shows computed impedance matching of waveguide terminated by broadband load and open end waveguide. It can be seen that septum-waveguide matching has a minor influence on total impedance matching. However waveguide termination has influence on port isolation (see Figure 10).

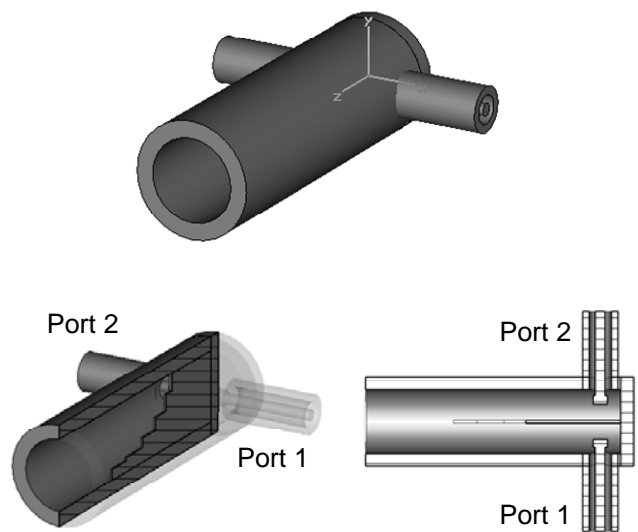


Figure 3: Designed septum waveguide for 47.0 – 48.5 GHz.

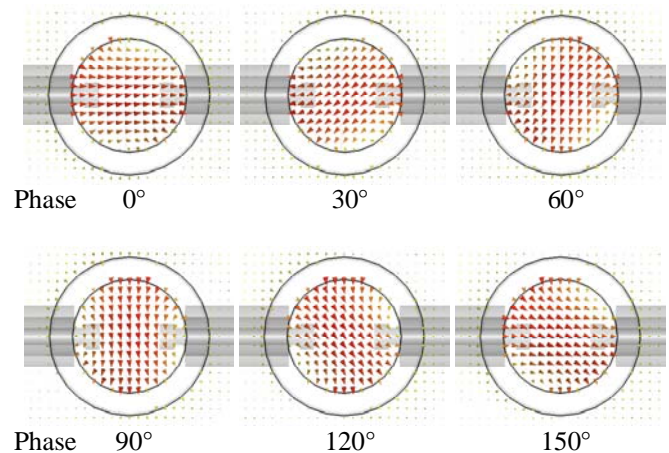
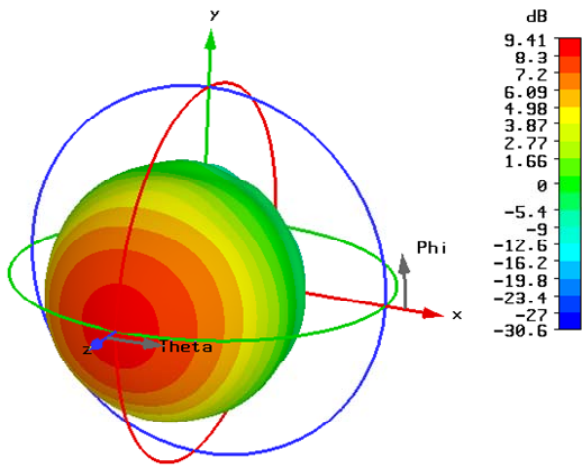


Figure 4: E-field shots showing phase rotation in circular waveguide caused by the septum - simulations.

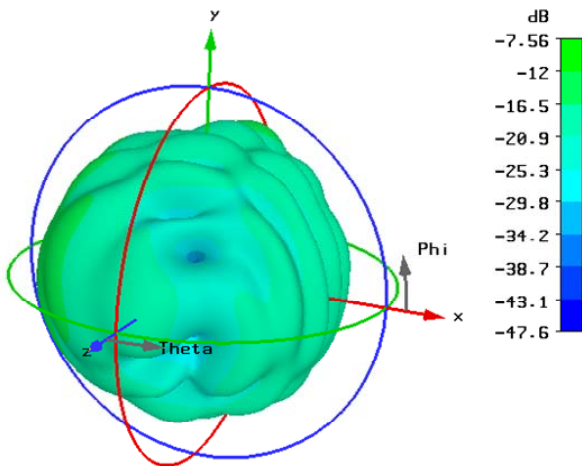
The creation of circular polarization by septum inside the waveguide is drawn in Figure 4 and Figure 5. Figure 4 shows E-field vector depending on signal phase. It is clearly seen that the vector is rotated across the waveguide. A good circularity for wide radiation angle is seen from axial ratio (AR) in Figure 5, (AR below 2 dB).

### 2.2 20 dB circular horn for 47 - 48.5 GHz frequency band

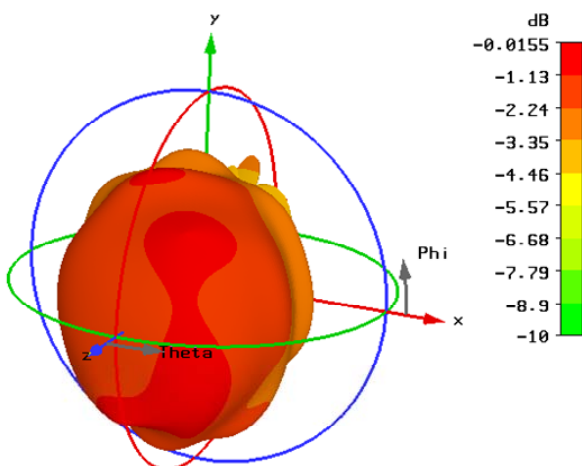
Design of circular horn issued from [6]. Figure 6 shows the designed 20 dB horn for 47 – 48.5 GHz frequency band. Horn length is 32 mm and aperture diameter is 26 mm. Horn with dimensions mentioned earlier was simulated in CST MWS. The horn antenna was excited with linearly polarized port mode  $TE_{11}$ . Calculated radiation patterns are shown in Figure 7, maximal calculated gain is 20 dB.



RH circular polarization



LH circular polarization



Axial Ratio

Figure 5: Septum waveguide farfield patterns, Port 1 excited - simulations.

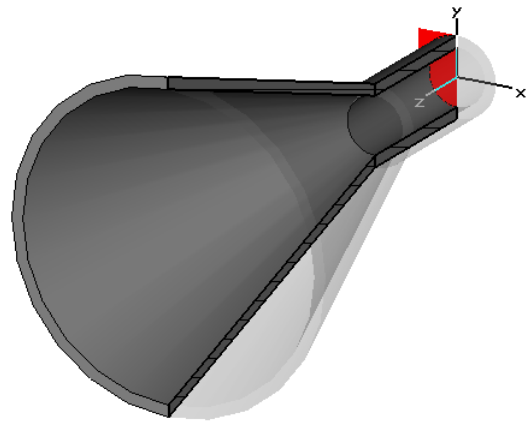


Figure 6: Designed 20 dB horn for 47.0 – 48.5 GHz.

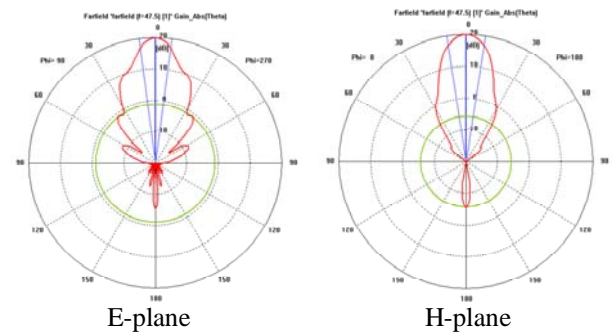
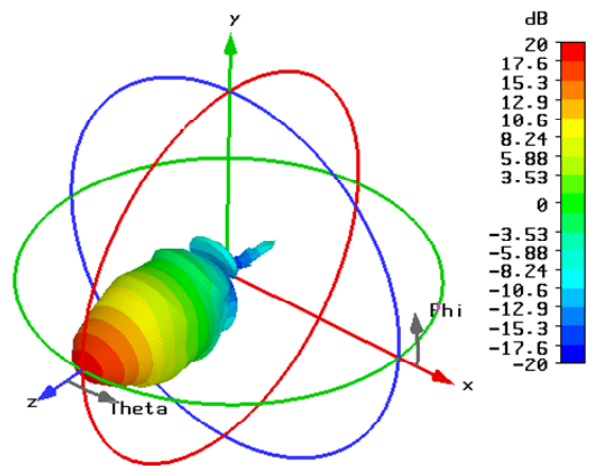


Figure 7: Farfield pattern of the horn excited with the  $TE_{11}$  mode – simulation.

### 2.3 20 dB septum horn simulations

Designed septum horn for 47 – 48.5 GHz frequency band is shown in Figure 8. Antenna consists of septum feed (Figure 3) and circular horn (Figure 6). The whole structure was analyzed with CST-MWS and computed data were evaluated. Figure 9 shows impedance matching. Matching is better than -20 dB from 43 GHz to 49 GHz. Port isolation is better than -25 dB between 46 GHz and 49 GHz. When we compare the

port isolation of septum and septum with horn, we can observe +5 dB better isolation between ports.

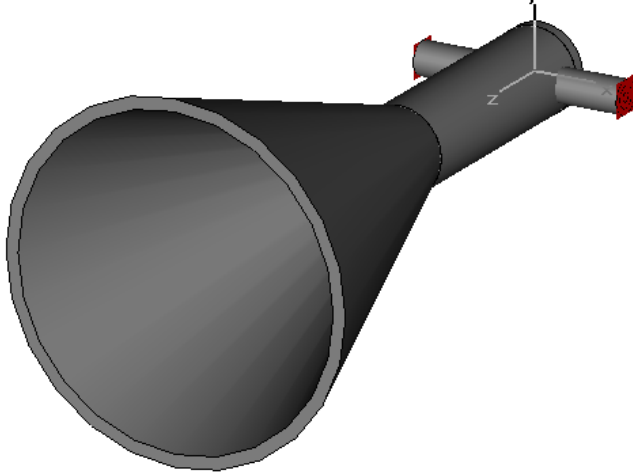


Figure 8: Designed septum horn for 47.0 – 48.5 GHz.

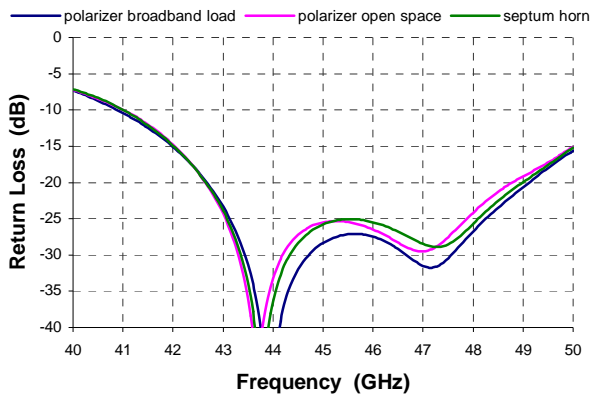


Figure 9: Impedance matching of polarizer with broadband load and with open space and septum horn – simulations.

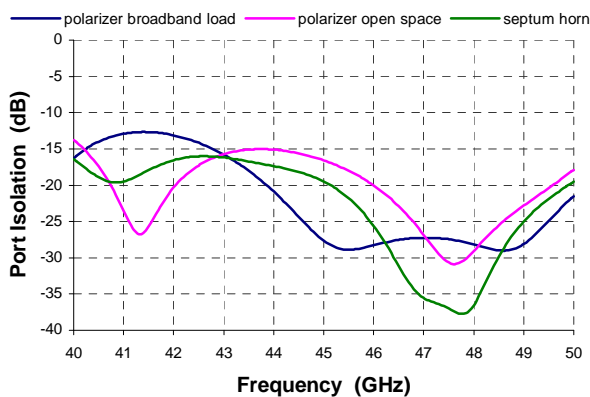


Figure 10: Port isolation of polarizer with broadband load and with open space and septum horn – simulations.

Radiation patterns at 47.5 GHz are shown in Figure 11. The gain of the horn is really 20 dB; that confirms results for excitation with linear polarization. In the case of circular

polarization the radiation pattern has an axial symmetry around the longitudinal axis (z) of the antenna (see Figure 11).

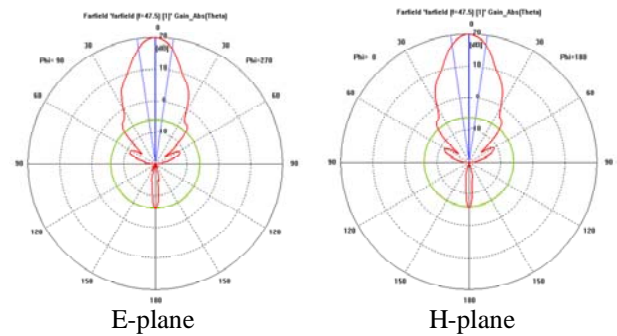
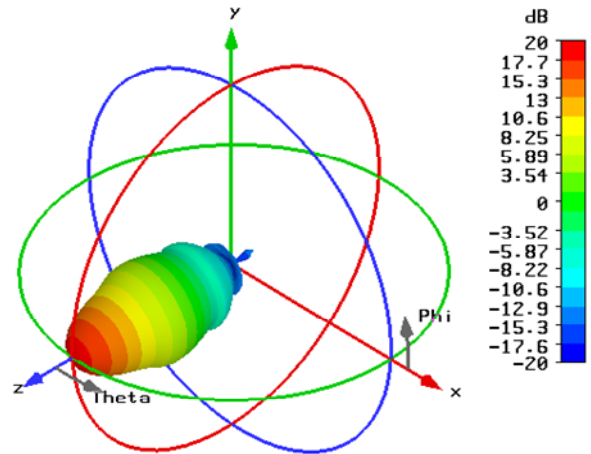


Figure 11: Septum horn farfield pattern at 47.5 GHz – simulation

Radiation pattern at 47.5 GHz are in the Figure 12 for the case of port 1 excitation (while port 2 has matched load). From the axial ratio values we can observe that polarization radiation properties are very sensitive to the radiation angle with its minimum (AR<0.5 dB) in the main lobe axis. Separation of the cross-polarization could be seen from Figure 13, where the principal cuts of the radiation pattern are drawn. Peak RHC and LHC spacing occurs along the z-axis again with value about 27 dB.

### 3 Design and measurement

Three antennas were design and manufactured (see Figure 14). Comparison of the measurement and simulation of matching of individual ports is in the Figure 15. We are able to see that the antenna fulfils all the specified criterions, however there is a slight difference between simulation and measurement. Figure 16 shows port isolations. Here is a good agreement of measurement and simulations, in the 47 - 48.5 GHz frequency is isolation better the -30 dB. Measured gains for co- and cross-polar polarization are shown in Figure 17 and Figure 18. Comparing measured and simulated results, measured gain is more then 0.5 dB lower and cross-polar level is also lower than simulated value. AR better then 0.7 dB was measured (see Figure 19).

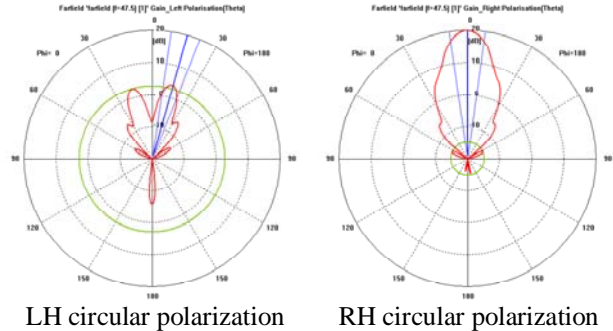
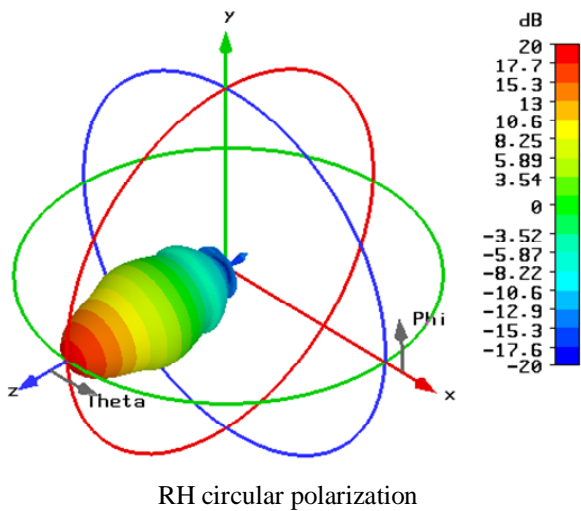


Figure 13: Septum horn farfield pattern at 47.5 GHz - simulation

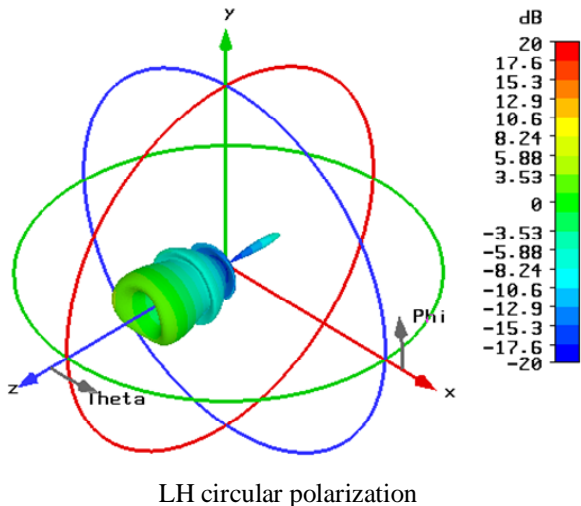


Figure 14: Realized 20 dBi gain septum horn antenna for 47.0 - 48.5 GHz frequency band.

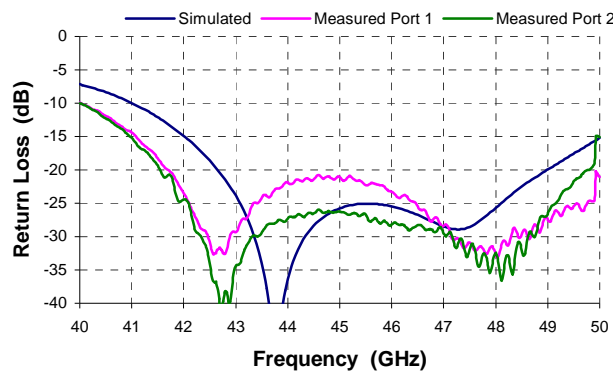
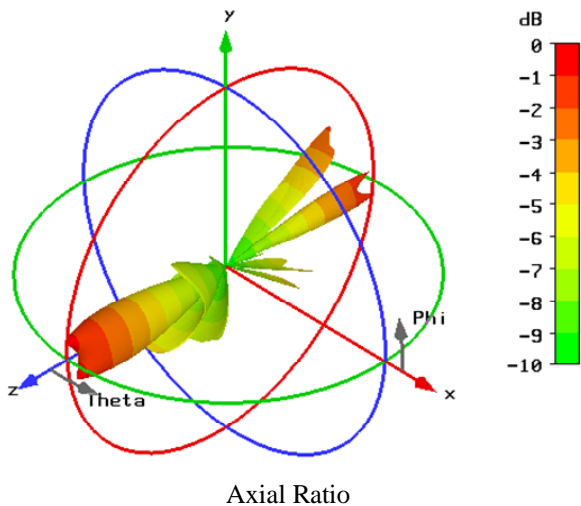


Figure 15: Comparison of simulated and measured septum horn impedance matching.

Figure 12: Septum horn farfield pattern at 47.5 GHz - simulations.

#### 4 Circular polarization and HAPs footprints

There are several possibilities which can improve power budget and capacity of communication via HAPs. Some of them are connected directly to the antennas (gain, pencil beam pattern, low sidelobes, polarization, footprint and its illumination etc.). The proper footprint illumination can be realized by the proper pre-distortion of the circular polarization (to the elliptical) to compensate the non-homogeneous site-footprint coverage. Straightforward solution is to use the circular-elliptical waveguide transition and to excite it in a circular part by two properly phase shifted signals with two orthogonal  $TE_{11}$  modes. Optimum phase-

shift of input signals for elliptical shape of the aperture is a function of geometrical dimensions of the elliptical aperture (axis fraction, wavelength).

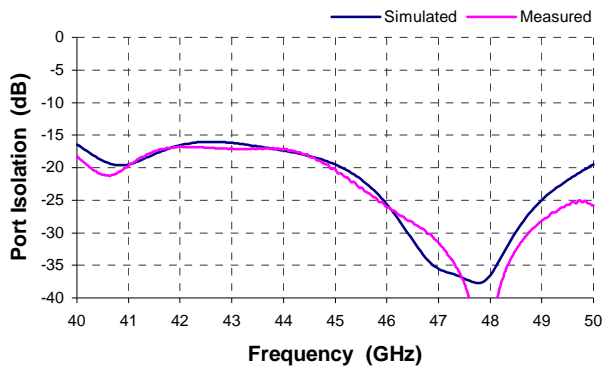


Figure 16: Comparison of simulated and measured septum horn port isolation - measured.

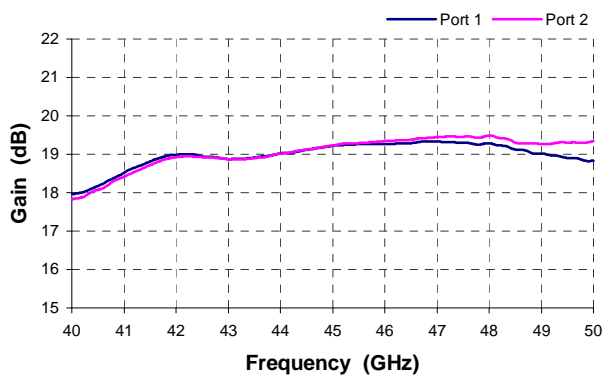


Figure 17: Septum horn gain (Polarization: Port 1 - RHC, Port 2 - LHC).

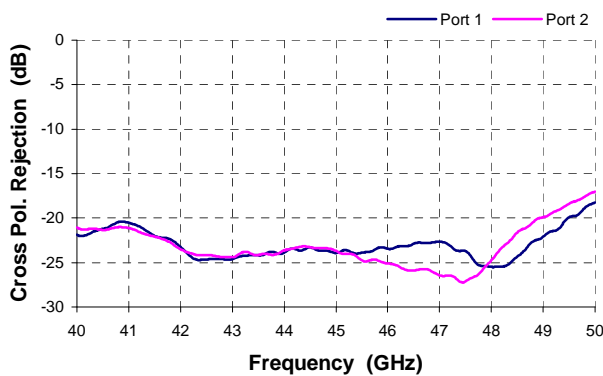


Figure 18: Septum horn cross polar rejection - measured.

## 5 Conclusion

Design and results of the septum horn antenna with two circular polarizations (LHC, RHC) and with high isolation between ports was described. Results for the 47/48 GHz band were presented. Possibility to optimize this design from the power budget and coverage point-of-view was mention too. The pre-distortion of the radiated field to compensate the elliptical footprints for HAPs was discussed as well.

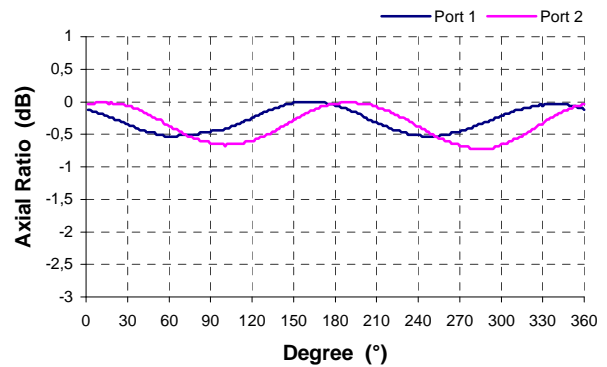


Figure 19: Septum horn axial ratio at 47.5 GHz (Port 1 - RHC, Port 2 - LHC) - measured.

## Acknowledgements

This research is a part of the international activities of the Antenna and Propagation group of the Department of Electromagnetic Field of the Czech Technical University in Prague in a frame of the Antenna Centre of Excellence (ACE2). Modelling was supported by the project of the Ministry of Education, Youth and Sports of the Czech Republic: Research in the Area of the Prospective Information and Navigation Technologies MSM 6840770014.

## References

- [1] U. Balaji, R. Vahldieck. "Field Theory Based S parameter Analysis of Circular Ridged Waveguide Discontinuities", IEEE XPLORE.
- [2] J. Bornemann, S. Amari, J. Uher, R. Vahldieck. "Fast and Efficient Mode-Matching Analysis of Ridged Circular Waveguide Polarizers", IEEE XPLORE.
- [3] M. H. Chen, G.N. Tsandoulas. "A Wide-Band Square-Waveguide Array Polarizer", IEEE Transactions on Antennas and Propagation, pp. 389-391, (1973).
- [4] G. M. Djuknic, J. Freidenfelds, Y. Okunev. "Establishing Wireless Communications Services via High-Altitude Aeronautical Platforms: A Concept Whose Time Has Come?", IEEE Commun. Mag., pp. 128-35, (1997).
- [5] P. Hazdra, R. Galuscak, M. Mazanek. "Optimization of th Septum Horn polarizer feed for 1.296 GHz EME Station", EuCAP 2006, (2006).
- [6] R. C. Johnson. "Antenna Engineering Handbook", McGraw-Hill, Inc., Chapter 15, (1993).
- [7] T. C. Tozer, D. Grace. "High-altitude platforms for wireless communications", IEE Electron. Commun. Eng. J., vol. 13, no. 3, pp.127-137, (2001).
- [8] Recommendation ITU-R F.1500, "Preferred Characteristics of Systems in the Fixed Service Using High-Altitude Platform Stations operating in the Bands 47.2-47.5 GHz and 47.9-48.2 GHz", International Telecommunications Union, (2000).
- [9] Mician GmbH web site: [www.mician.com](http://www.mician.com)